Immunogold Electron Microscopy of Phytochrome in *Avena*: Identification of Intracellular Sites Responsible for Phytochrome Sequestering and Enhanced Pelletability

David W. McCurdy and Lee H. Pratt

Department of Botany, University of Georgia, Athens, Georgia 30602. Dr. McCurdy's present address is Department of Developmental Biology, Research School of Biological Sciences, The Australian National University, Canberra, Australia.

Abstract. Using monoclonal antibodies to the plant photoreceptor, phytochrome, we have investigated by immunogold electron microscopy the rapid, red light–induced, intracellular redistribution (termed "sequestering") of phytochrome in dark-grown *Avena* coleoptiles. Pre-embedding immunolabeling of 5-μm-thick cryosections reveals that sequestered phytochrome is associated with numerous, discrete structures of similar morphology. Specific labeling of these structures was also achieved by post-embedding ("on-grid") immunostaining of LR-White–embedded tissue, regardless of whether the tissue had been fixed chemically or by freeze substitution. The phytochrome-associated structures are globular to oval in shape, 200–400 nm in size, and are composed of amorphous, granular material. No morphologically identifiable membranes are present either surrounding or within these structures, which are often present as apparent aggregates that approach several micrometers in size.

An immunogold labeling procedure has also been developed to identify the particulate, subcellular component with which phytochrome is associated in vitro as a consequence of irradiation of *Avena* coleoptiles before their homogenization. Structures with appearance similar to those identified in situ are the only components of the pelletable material that are specifically labeled with gold. We conclude that the association of phytochrome with these structures in *Avena* represents the underlying molecular event that ultimately is expressed both as red light–induced sequestering in vivo and enhanced pelletability of phytochrome detected in vitro.

PHYTOCHROME is a plant chromoprotein that regulates many photomorphogenic responses of plants to light (24). The native protein is a dimer of two identical, ~120-kD monomers, each with one linear, tetrapyrrole chromophore (see reference 8). Phytochrome exists in either the physiologically inactive, red-absorbing form (Pr, A_{max} near 665 nm)[1], or the physiologically active, far red–absorbing form (Pfr, A_{max} near 730 nm).

Phytochrome is synthesized de novo as Pr, which is the form that accumulates in seedlings that are grown in darkness. Photomorphogenic activity results from absorption of light by Pr, which converts it to the active, Pfr form. This induction of photomorphogenic responses in plants by red (R) light can be cancelled by subsequent irradiation with far red (FR) light, which converts Pfr back to Pr. The photobiology of phytochrome has been reviewed extensively (see reference 24).

The molecular mechanism(s) by which phytochrome controls photomorphogenic responses in plants is unknown. The bulk of the phytochrome that is present in crude extracts of dark-grown tissue displays biochemical properties that are typical of a water-soluble protein (12). After photoconversion of Pr to Pfr in vivo, however, as much as 80% of the spectrally detectable phytochrome can be in pelletable fractions isolated from such crude extracts (21). This preferential association of Pfr with particulate, subcellular material led to speculation that the chromoprotein might be reacting with a Pfr-specific receptor in the cell, and that among other possibilities such binding might represent an initial event in the mode of action of the photoreceptor (for reviews see 10, 12).

Independently, a preferential association of Pfr with one or more previously unidentified subcellular components has been demonstrated in vivo by immunocytochemistry (9). Pr exhibits a diffuse distribution throughout the cytosol in cells that have never been exposed to light, whereas Pfr is associated with numerous discrete regions throughout the cell. This R light–dependent redistribution of phytochrome, which has been termed "sequestering" (9), has been detected in several monocotyledonous plants (7), as well as in a dicotyledonous plant (23). In *Avena*, phytochrome sequestering displays characteristics similar to those for enhanced pelletability of Pfr. In particular, both processes are completed at

1. *Abbreviations used in this paper*: FR, far red; GAR, goat antibodies to rabbit IgG; PAS, phytochrome-associated structure; Pr and Pfr, red- and far red–absorbing forms of phytochrome, respectively; R, red; RAM, rabbit antibodies to mouse IgG; TBS, Tris-buffered saline.

room temperature within 10 s after the formation of Pfr (11, 16), and both exhibit similar temperature dependence (11, 16, 20).

Attempts to identify the subcellular sites with which Pfr associates as a consequence of its enhanced pelletability and of sequestering have been unsuccessful. High levels of divalent cations (10 mM) are required in extraction buffers to sustain enhanced pelletability in vitro, but at these concentrations cations also induce aggregation of membranes and nucleic acids so that conventional separation techniques, such as sucrose density gradient centrifugation, are rendered unsuitable (18). Immunoelectron microscopy using ultrathin frozen sections has been used in combination with ferritin-labeled antibodies to examine sequestered phytochrome in *Avena* coleoptiles (27). In this case, however, less than optimal structural preservation of the tissue limited the value of the observations.

Identification of the intracellular sites with which phytochrome associates as a consequence of sequestering and of enhanced pelletability represents the major unresolved question concerning both phenomena. Their identification might also determine unambiguously whether sequestering and enhanced pelletability are manifestations of the same basic phenomenon. We report here the use of immunogold electron microscopy to identify the structures with which *Avena* phytochrome is associated both in situ in coleoptiles and in vitro in the pelletable fraction from light-treated coleoptile tissue.

Materials and Methods

Plant Tissue and Light Treatments

Oats (*Avena sativa* L., cv. Garry) were grown in darkness on cellulose packing material at 25°C in saturating humidity for 3–4 d. For immunocytochemical observations of light-treated tissue, the apical 3–4 cm of intact coleoptiles were irradiated with short, saturating pulses of R and FR light using a custom-built, 500-W light source (11). R light was obtained with a Balzers B-40, 665-nm interference filter (Balzers S. p. A., Liechtenstein) and FR light with a Plexiglas FRF-700 cutoff filter (Westlake Plastics Co., Lenni, PA). Immediately after the appropriate light treatment, coleoptiles were split longitudinally and apical 3–5-mm pieces were placed in fixative. "Dark" tissue was processed similarly but never exposed to R or FR light.

For experiments involving the immunolabeling of phytochrome in pelleted crude extracts, whole seedlings were irradiated for 5 min with a light source consisting of a bank of six unfiltered 40-W Gro-Lux lamps (Sylvania, Danvers, MA). This light source establishes within 5 s a photostationary equilibrium for phytochrome that is indistinguishable from that produced by monochromatic R light (1). FR light for this application was obtained by filtering the output of a tungsten microscope illuminator (Unitron LKR, Unitron Instruments Inc., Plainview, NY) with a Plexiglas FRF-700 cutoff filter.

Until the various fixations were complete, tissue and tissue extracts were handled under green safe light that phytochrome does not absorb (14).

Phytochrome Spectral Assay

Phytochrome photoreversibility was measured in crude extracts at 660 vs. 730 nm with a custom-built, dual-wavelength spectrophotometer (17). Samples of 0.4 ml were mixed with 0.5 g of $CaCO_3$, which acts as a light scattering agent and thereby enhances absorbance values (2).

Conventional Electron Microscopy

Coleoptile pieces were fixed overnight on ice with 2% (vol/vol) glutaraldehyde in 0.1 M sodium phosphate, pH 7.4. The tissue was rinsed twice in 0.1 M sodium phosphate, pH 7.4, postfixed for 2 h in 2% (wt/vol) aqueous OsO_4, washed again with 0.1 M sodium phosphate, pH 7.4, and processed through a cold ethanol series before being embedded in Spurr's resin. Silver-gold sections were picked up onto formvar-coated copper grids and stained with 5% (wt/vol) aqueous uranyl acetate and Reynold's lead citrate. Sections, including those for all the immunolabeling experiments, were viewed with a Zeiss 10A electron microscope operated at 60 kV.

Antibodies

Unless otherwise indicated, all antibodies were diluted in PBS (10 mM sodium phosphate, 140 mM NaCl, pH 7.4) containing 10% (vol/vol) lamb serum (Gibco, Grand Island, NY) and 0.02% (wt/vol) NaN_3. The three monoclonal antibodies (Oat-13, Oat-22, Oat-25) used here were selected from a panel of antibodies raised against phytochrome purified from dark-grown *Avena* shoots (4, 5). All were immunopurified from hybridoma medium with a column of immobilized rabbit antibodies to mouse IgG (RAM) (5). Oat-13 is an IgG2a, while Oat-22 and Oat-25 are IgG1s (4). Each antibody has been determined to be immunocytochemically competent (our unpublished observations), and each recognizes an independent epitope on phytochrome (4).

Immunopurified rabbit antibodies to mouse IgGs (RAMs) were prepared as described previously (5). Rhodamine was conjugated to goat antibodies to rabbit IgG (2612-0081, Cappel Scientific, Div. of CooperBiomedical, Melbourne, PA). Goat antibodies to rabbit IgG (GAR; R-2004, Sigma Chemical Co., St. Louis, MO) were coupled to 5-nm colloidal gold particles (Janssen G-5, SPI Supplies, West Chester, PA) according to the method of De Mey et al. (6), as modified by Raikhel et al. (22). The gold-labeled antibodies were resuspended in PBS containing 10% (vol/vol) lamb serum and 0.02% (wt/vol) polyethylene glycol (20,000 mol wt; Sigma Chemical Co.) to make a final antibody concentration of ~35 μg/ml. For some experiments, GAR coupled to 20-nm colloidal gold (GAR 20, Janssen Pharmaceutica, Beerse, Belgium) was used at a 1:2 dilution with PBS containing 10% (vol/vol) lamb serum. Non-immune mouse IgG was from Sigma Chemical Co. (I-5381).

Immunofluorescence Microscopy

All procedures for immunofluorescence microscopy of 1-μm-thick cryosections of coleoptile tissue were performed as described previously (11).

Pre-embedding Immunoelectron Microscopy

Tissue was fixed on ice for 24 h with 4% (wt/vol) freshly prepared formaldehyde in 0.1 M sodium phosphate, pH 7.4. Fixed tissue was infiltrated first for 8 h at 4°C with 1.0 M sucrose in 0.1 M sodium phosphate, pH 7.4, containing 0.4% (wt/vol) formaldehyde, and then for 4–6 h at 4°C with 1.3 M sucrose in 0.1 M sodium phosphate, pH 7.4. These conditions of fixation and sucrose infiltration caused some plasmolysis of the tissue. Reducing the osmolarity of the fixation buffer, however, did not appreciably reduce this problem with the coleoptile tissue examined here. Cryosections (5–6 μm thick), which were cut with a Sorval FTS-Cryosectioning apparatus operated at −45°C, were transferred to silicone-treated glass slides. Sections were immunolabeled as previously described (11), except that antibody incubations were for 2 h and the final antibody was GAR-colloidal gold. Control sections were treated identically except that an equivalent concentration of non-immune mouse IgG replaced the mixture of monoclonal antibodies. After extensive washing with PBS, the immunolabeled sections were refixed with 2% (wt/vol) glutaraldehyde in 0.1 M sodium phosphate, pH 7.4, postfixed with 2% (wt/vol) OsO_4, dehydrated with ethanol, and infiltrated with Spurr's resin. The sections, which were still on the glass slides, were inverted and placed in contact with plastic capsules filled with Spurr's resin. After polymerization, the resin with attached section was separated from the glass surface. Silver-gold sections cut from the surface of these re-embedded cryosections were stained with uranyl acetate and lead citrate as above.

Post-embedding Immunoelectron Microscopy

Fixation was for 24 h on ice with 4% (wt/vol) freshly prepared formaldehyde and 0.5% (vol/vol) glutaraldehyde in 0.1 M sodium phosphate, pH 7.4. After washing with two changes of ice-cold 0.1 M sodium phosphate, pH 7.4, and dehydrating through a cold ethanol series, the fixed tissue was infiltrated over a 24-h period at 4°C with LR-White resin (Polysciences, Inc., Warrington, PA). Polymerization was at 62°C for 24 h. Silver sections were picked up with formvar-coated nickel grids and processed for on-grid immunolabeling as follows: 30 min in Tris-buffered saline (TBS) containing BSA (TBS–BSA: 10 mM Tris–HCl, 500 mM NaCl, 0.3% [vol/vol] Tween-20, 1% [wt/vol] BSA) and 5% [vol/vol] lamb serum; 1 h in a mixture of

all three monoclonal antibodies to phytochrome (each at 5 μg/ml in TBS–BSA plus 1% [vol/vol] lamb serum); three 10-min washes with TBS–BSA; 1 h in RAM (5 μg/ml in TBS–BSA plus 1% [vol/vol] lamb serum); three 10-min washes with TBS–BSA; 1 h in GAR coupled with 5-nm colloidal gold (1:1 dilution of the 35 μg/ml preparation with TBS–BSA containing 1% [vol/vol] lamb serum). Final washing was for 10 min in TBS, followed by three 10-min washes in deionized and distilled H_2O. Nonimmune mouse IgG (15 μg/ml in TBS–BSA plus 1% [vol/vol] lamb serum) was used in place of the monoclonal antibodies for control sections. The sections were stained with uranyl acetate and lead citrate.

Freeze Substitution Fixation and Immunoelectron Microscopy

Coleoptile pieces held with forceps were rapidly plunged into liquid propane that was cooled by a surrounding jacket of liquid nitrogen. After 5–6 s, the tissue was quickly transferred to plastic bottles containing anhydrous acetone held at liquid nitrogen temperature. The bottles were buried in dry ice and stored at −80°C for 3 d. The acetone-substituted tissue was brought to room temperature over a 24-h period and washed at this temperature with three changes of anhydrous ethanol before infiltration with LR-White resin. Silver sections cut from the polymerized blocks were processed for on-grid immunolabeling as described above.

Immunolabeling In Vitro

After appropriate light treatments, 2-g lots of chilled coleoptile tissue were extracted with an ice-chilled mortar and pestle into 6 ml of extraction buffer (35 mM 3-[*N*-morpholino]propanesulfonic acid, 10 mM $MgSO_4$, 3 mM Na_4EDTA, 250 mM sucrose, 14 mM 2-mercaptoethanol, and 0.1% [wt/vol] BSA, pH adjusted to 7.6 with NaOH). The extracts were passed through Miracloth and centrifuged at 14,600 *g* for 15 min at 4°C. The pelleted material was resuspended into a volume of extraction buffer equal to that of the recovered supernatant. Aliquots of both the supernatant and resuspended pellet were taken for spectral assay of phytochrome.

The resuspended pellet was held on ice for 1 h, irradiated on ice for 5 min with FR light, divided into equal aliquots and centrifuged again at 14,600 *g*, 4°C, for 15 min. One pellet was resuspended with extraction buffer and assayed spectrophotometrically to verify that phytochrome remained associated with the particulate material after the above treatment. The other pellet was gently resuspended into ice-cold 0.1 M sodium phosphate, pH 7.4, 10 mM $MgSO_4$, 250 mM sucrose, 4% (wt/vol) freshly prepared formaldehyde, and fixed overnight on ice. The fixed material was pelleted into 1% (wt/vol) low gelling temperature agarose (Type VII; Sigma Chemical Co.) at 32°C. The agarose was then gelled by reducing the temperature to 4°C. The gelled pellet was sliced into 1-mm^3 blocks. Blocks were washed for 30 min in PBS followed by 1 h in undiluted lamb serum, after which

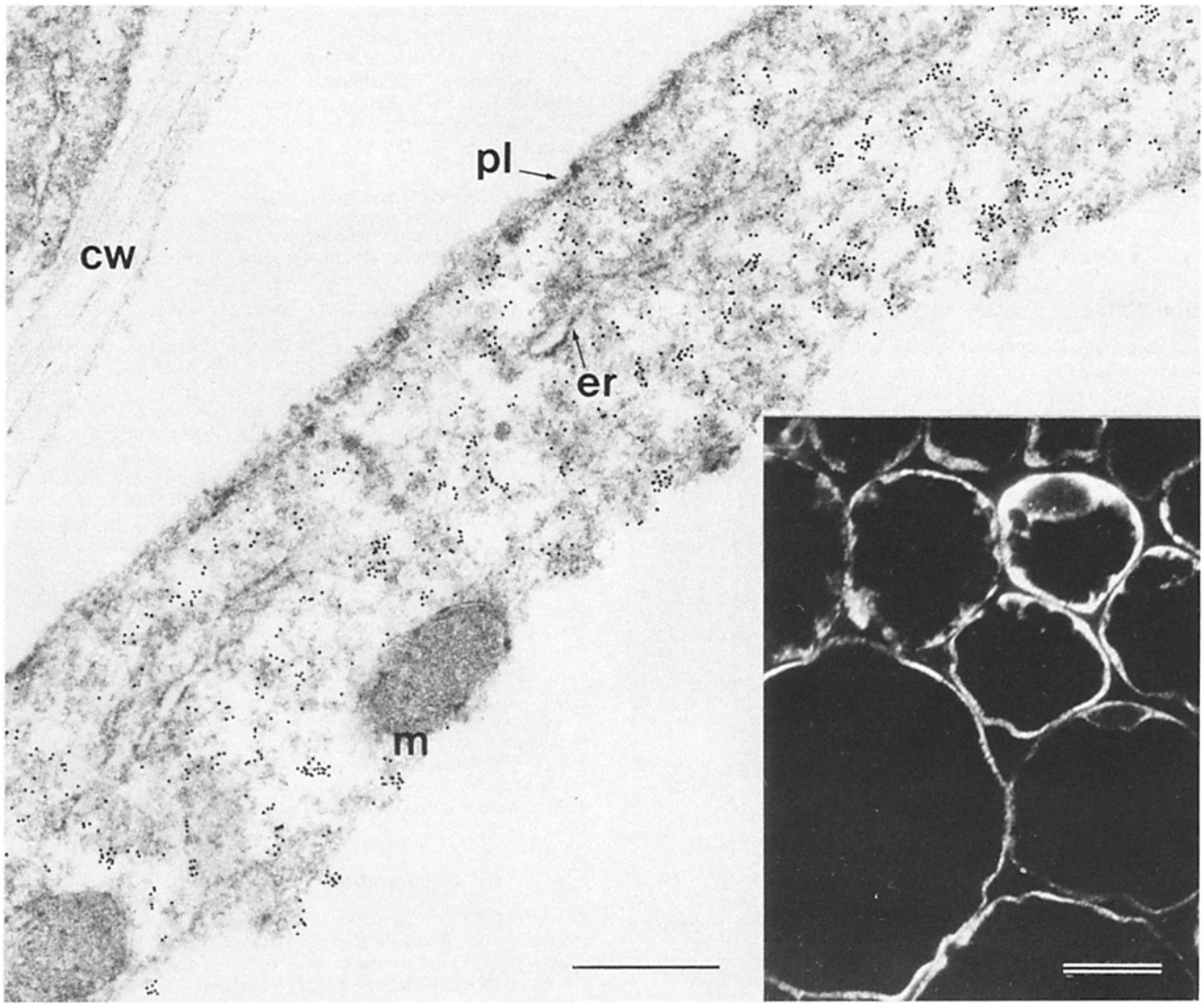

Figure 1. Pre-embedding immunogold localization of phytochrome as Pr in dark-grown, non-irradiated *Avena* coleoptile tissue. Phytochrome-specific immunolabel (20-nm colloidal gold) is diffusely distributed throughout the cytosol and is not associated with endoplasmic reticulum (*er*), mitochondria (*m*), or the plasmalemma (*pl*), which in this case has withdrawn from the cell wall (*cw*) due to plasmolysis. Bar, 0.5 μm. (*Inset*) Immunofluorescence localization of phytochrome showing the diffuse, cytosolic distribution of this pigment as observed at the light microscope level. Bar, 20 μm.

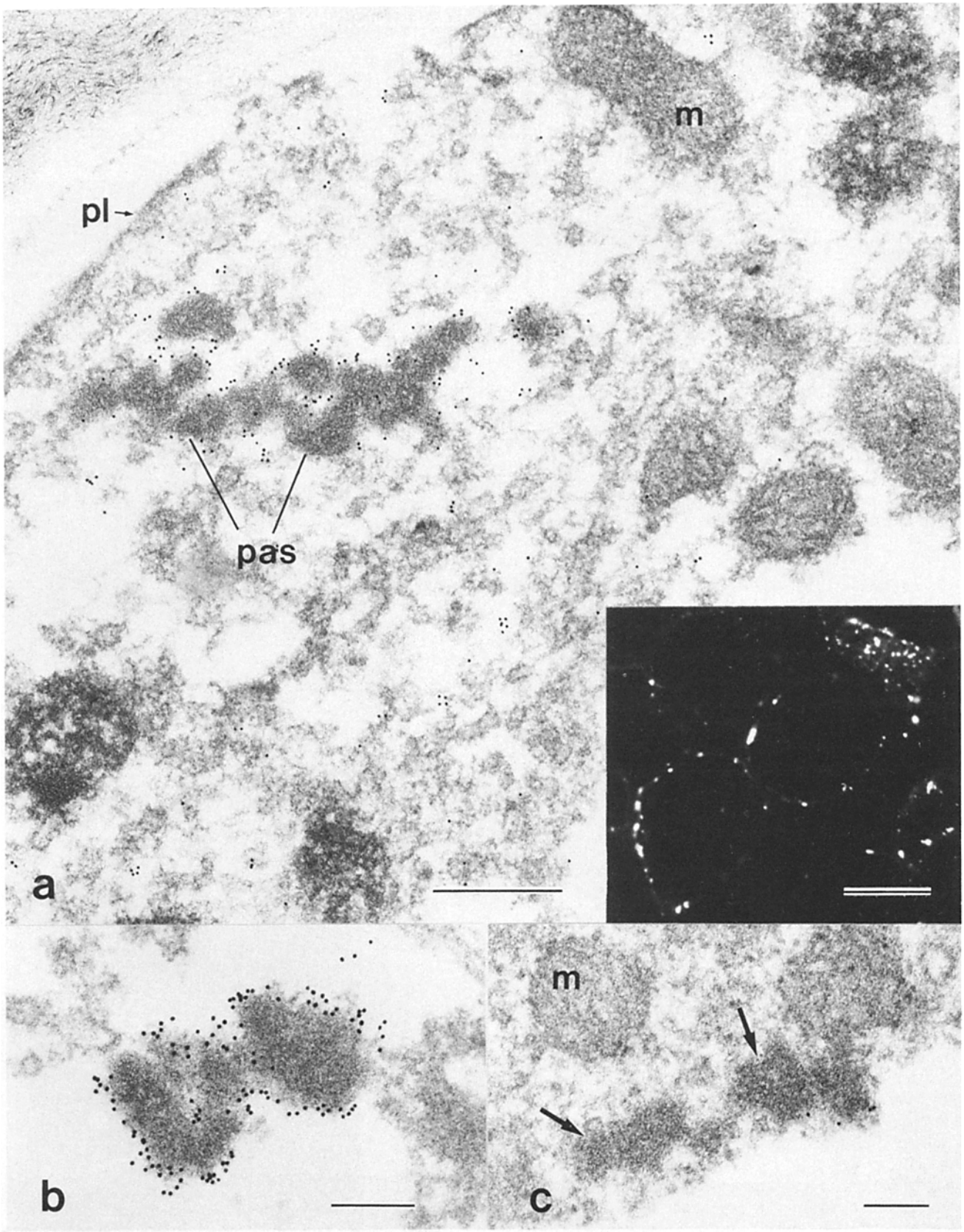

Figure 2. Pre-embedding immunogold localization of phytochrome as Pfr in dark-grown, R/FR-irradiated *Avena* coleoptile tissue. (*a*) Phytochrome-specific immunolabel (20-nm colloidal gold) is associated with the PASs (*pas*); no immunolabel is found in association with mitochondria (*m*) or the plasmalemma (*pl*). Bar, 0.5 μm. (*Inset*) Immunofluorescence localization of phytochrome showing the sequestered distribution of this pigment as observed at the light microscope level. Bar, 20 μm. (*b*) Higher magnification view of two PASs. Bar, 0.2 μm. (*c*) Control section incubated with non-immune mouse IgG. The PASs (*arrows*) are not labeled with colloidal gold. *m* denotes a mitochondrion. Bar, 0.2 μm.

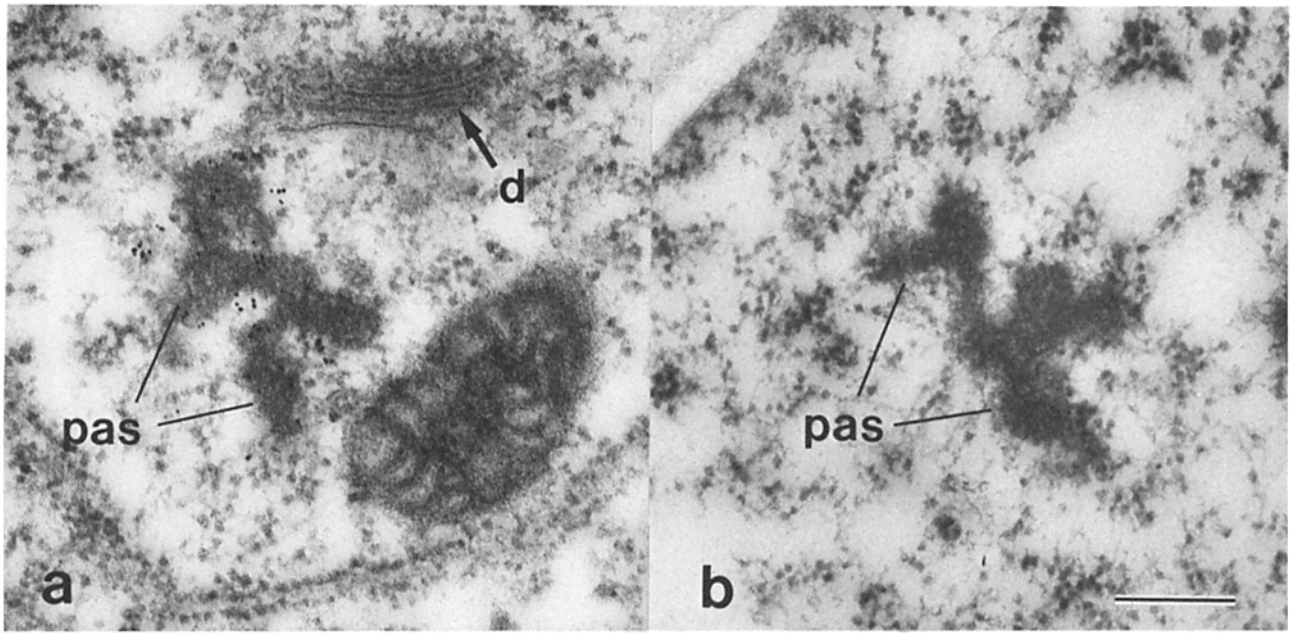

Figure 3. Post-embedding immunogold labeling of phytochrome as Pfr in R/FR-irradiated *Avena* coleoptile tissue. (*a*) PASs (*pas*) labeled with 5-nm colloidal gold. Note that the colloidal gold is smaller and more electron dense than the numerous ribosomes. The dictyosome (*d*) is not immunolabeled. Bar, 0.2 μm. (*b*) Control section incubated with non-immune mouse IgG. The PASs (*pas*) are not immunolabeled. Bar, 0.2 μm.

they were incubated overnight at 4°C in 100 μl of a mixture of the three monoclonal antibodies to oat phytochrome, each at 10 μg/ml. Control blocks were incubated in 100 μl of 30 μg/ml non-immune mouse IgG. Immunolabeled blocks were washed with two changes of PBS containing 10% (vol/vol) lamb serum over a period of 1 h, followed by two 30-min incubations in undiluted lamb serum. Washed blocks were incubated in 10 μg/ml RAM for 2 h at room temperature, after which they were washed as before. Finally, blocks were incubated for 2 h at room temperature in GAR-colloidal gold (5 nm). After washing overnight in PBS, the blocks were re-fixed with 2% (vol/vol) glutaraldehyde in 0.1 M sodium phosphate, pH 7.4, postfixed with 2% (wt/vol) OsO_4, dehydrated through an ethanol series, and embedded in Spurr's resin. Silver-gold sections were stained with uranyl acetate and lead citrate as above.

Carbohydrate-specific Cytochemical Staining

Silver–gold sections of the pelleted, immunolabeled material from light-treated coleoptile tissue were picked up on gold grids and stained for the presence of carbohydrates with periodic acid, thiocarbohydrazide, and silver protein (Polysciences, Inc.) using the method of Thiéry (26) as modified by Taylor and Fuller (25). Sections were viewed without uranyl acetate or lead citrate staining.

Results

All in situ observations of light-treated tissue reported here are of *Avena* coleoptiles that have been treated in vivo with 1 s R light, 10 s darkness, and 4 s FR light. Previous work using immunofluorescence microscopy demonstrated that this sequence of irradiation, referred to throughout as R/FR-irradiation, results in essentially all of the immunodetectable phytochrome being in the sequestered condition (11). Furthermore, because the apparent aggregation of loci of sequestered phytochrome is dependent upon the continued presence of Pfr within the cell (11), the terminal pulse of FR light, which converts Pfr back to Pr, enables relatively precise control of the extent of the overall sequestering process. Thus, all immunocytochemical observations reported here are of R/FR-irradiated tissue that exhibit comparable stages of sequestering.

Intracellular Distribution of Sequestered Phytochrome as Detected by Pre-embedding Immunoelectron Microscopy

Ultrathin sections of 5-μm thick, immunogold-labeled, re-embedded cryosections reveals a general cytosolic distribution of phytochrome as Pr in dark-grown, non-irradiated tissue (Fig. 1). No association of phytochrome with any particular organelle or membrane is detected. The general cytosolic distribution seen here at the electron microscope level is consistent with the overall diffuse distribution seen previously (11) by immunofluorescence microscopy (Fig. 1, inset). In contrast, however, most of the immunolabel in R/FR-irradiated tissue is associated with discrete, amorphous structures that lack any readily identifiable morphology (Fig. 2). This preferential association of immunolabel with discrete, cytoplasmic structures is consistent with observations made at the immunofluorescence level (11) for R/FR-irradiated tissue (Fig. 2 *a*, inset). These amorphous entities, which we have termed phytochrome-associated structures (PASs), are present either as globular or roughly oval-shaped units of ~200–400 nm in size (Fig. 2 *b*). More frequently, however, the PASs are present as irregularly shaped, apparent aggregates of the presumed unit structures (Fig. 2 *a*). Control tissue treated with non-immune mouse IgG shows no labeling of the PASs (Fig. 2 *c*).

Post-embedding Immunogold Labeling of Sequestered Phytochrome

In LR-White sections of R/FR-irradiated tissue, only amorphous structures with appearance similar to the PASs seen in Fig. 2 are labeled after "on-grid" immunolabeling (Fig. 3 *a*). The colloidal gold in this case is in part superimposed upon these structures, rather than being located exclusively at the edges of the PASs as observed after pre-embedding immunolabeling (Fig. 2). Immunolabel is absent from or-

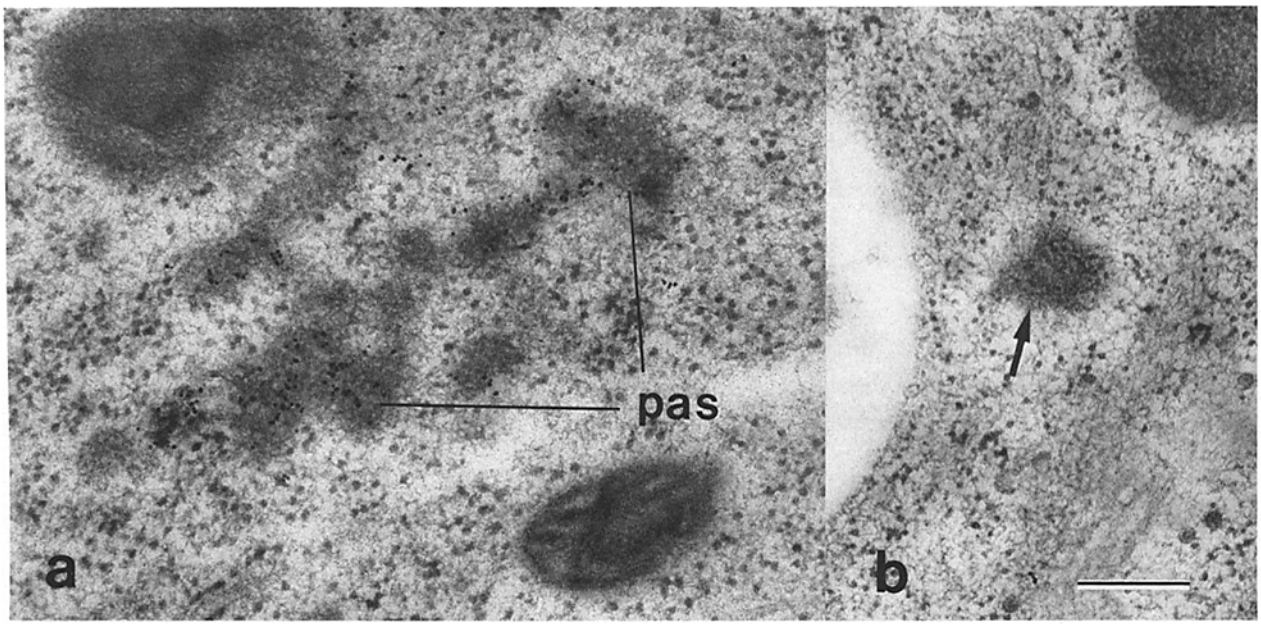

Figure 4. Post-embedding immunogold labeling of phytochrome as Pfr in R/FR-irradiated *Avena* coleoptile tissue that has been fixed by freeze substitution. (*a*) PASs (*pas*) labeled with 5-nm colloidal gold. The colloidal gold is smaller and more electron dense than the surrounding ribosomes. (*b*) Control section incubated with non-immune mouse IgG. The PASs (*arrow*) are not labeled with gold. Bar, 0.2 μm.

ganelles such as microbodies (data not shown), mitochondria, endoplasmic reticulum, and dictyosomes (Fig. 3 *a*). Both the individual structures (data not shown) and the larger, apparent aggregates of these PASs (Fig. 3 *a*) are present in these sections. Non-immune mouse IgG, when substituted for the phytochrome-specific monoclonal antibodies, does not label these PASs (Fig. 3 *b*).

Freeze Substitution Fixation and Immunolabeling of Phytochrome-associated Structures

Structures similar to those identified above are present and are labeled with gold in R/FR-irradiated tissue that had been fixed by freeze substitution and embedded in LR-White resin (Fig. 4). Individual PASs (data not shown) and apparent aggregates of these structures (Fig. 4 *a*) are observed in this tissue. Immunolabeling of the PASs is absent in sections of R/FR-irradiated tissue that had been treated with non-immune mouse IgG (Fig. 4 *b*). Some localized freezing damage occurs throughout the cytoplasm as a result of the freeze substitution fixation, but it does not obscure identification of the PASs or other organelles present in these cells.

Phytochrome-associated Structures in Avena Coleoptiles Prepared for Conventional Electron Microscopy

Amorphous structures similar in appearance to the PASs identified by immunogold labeling are distributed throughout the cytosol of epidermal and parenchymal cells of R/FR-irradiated tissue fixed and processed for conventional electron microscopy (Fig. 5). Consistent with the immunolabeled material, the PASs are usually observed to be clustered together (Fig. 5), often with several smaller PASs in close proximity (Fig. 5, arrows). Serial sectioning (data not shown) indicated that these smaller, peripheral structures were not connected to the larger groups of the PASs. These structures are not surrounded by a morphologically identifiable membrane, and their contents are granular in appearance (Fig. 5, inset). The aggregates are often located in areas of more abundant cytoplasm, such as in the corners of the cells or adjacent to larger organelles such as nuclei or plastids. Overall, however, no preferential association of these structures with any particular cell component or location was seen.

Immunolabeling In Vitro of Pelletable Phytochrome in Crude Extracts of Light-treated Coleoptile Tissue

As before (16), following the photoconversion in vivo of phytochrome to its active, Pfr form, an ~12-fold increase in the amount of spectrally detectable pigment is observed in the pelletable fraction from a crude extract of dark-grown *Avena* coleoptiles (Table I). Structures resembling the PASs seen in situ are the only components that are specifically labeled with gold after immunolabeling in vitro of these pelleted fractions (Fig. 6). These structures are 200–300 nm in size and are present in the pelleted material either as individual entities (Fig. 6, arrows), or as larger, apparent aggregates of these structures (Fig. 6). The amorphous contents of these structures are very similar in appearance to the PASs immunolabeled in situ (Fig. 2 *b*). Neither these structures nor any other components of the pelleted material were immunolabeled after incubation in non-immune mouse IgG (Fig. 6, inset).

Cytochemical Analysis of the Pelletable Phytochrome-associated Structures

The pelletable PASs do not react positively when tested for the presence of carbohydrate (Fig. 7). Other components of the pelleted material, however, develop electron-dense staining that is characteristic of the presence of carbohydrate (Fig. 7, arrow).

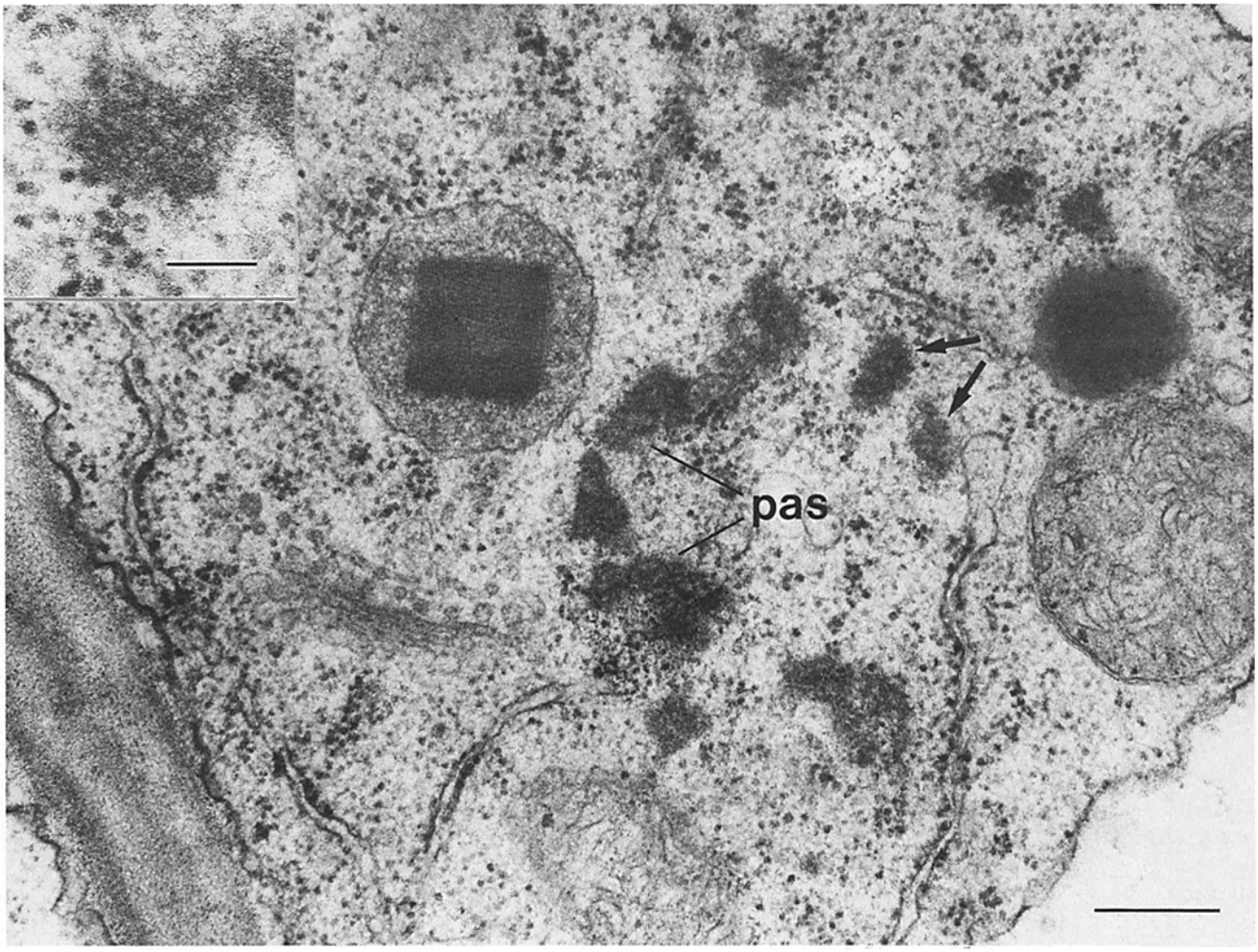

Figure 5. Electron micrograph of R/FR-irradiated *Avena* coleoptile tissue processed for conventional electron microscopy. The PASs (*pas*) form apparent aggregates that are often surrounded by individual PASs (*arrows*). Bar, 0.3 μm. (*Inset*) Higher magnification view of a PAS. Bar, 0.1 μm.

Discussion

As observed previously (7, 9), phytochrome as Pr is distributed diffusely throughout the cytosol in a manner that is consistent with a water-soluble protein (Fig. 1). In contrast, following photoconversion to its active, Pfr form, phytochrome is observed in association with discrete, amorphous PASs that are distributed throughout the cytosol of epidermal and parenchymal cells (Figs. 2–4). In R/FR-irradiated tissue, individual PASs are often observed in close proximity to tight clusters of two or three PASs (Figs. 2 *a*, 3*a*, 5). Such a configuration is consistent with the suggestion that the PASs may be in the process of aggregating (11). Similarly, pelleted phytochrome is associated with particulate structures that appear to be identical to those recognized in situ (compare Fig. 2 *b* to Fig. 6). Furthermore, these structures are present in the pelletable fractions as either individual entities or as apparent aggregates (Fig. 6), a situation that again matches that seen in situ. Thus, the morphological evidence presented here indicates that the PASs seen in vivo are the same structures as those seen in situ. These observations provide direct evidence that both enhanced pelletability and intracellular sequestering are different manifestations of the same intracellular event(s).

The specificity of the immunolabeling for phytochrome can be inferred from the following considerations. (*a*) Each of the three monoclonal antibodies used here has previously been demonstrated to be directed to, and specific for, phytochrome isolated from dark-grown *Avena* shoots (4, 5). (*b*) In all instances, parallel controls using non-immune mouse IgG, which is more rigorous than simply omitting the primary antibody, demonstrated that there was no nonspecific binding by the second and third antibodies that were used in the immunolabeling protocols. (*c*) Each of the three monoclonal antibodies gave identical results when used indi-

Table I. Dual-Wavelength Photoreversibility Measurements of Phytochrome Pelletability in Crude Extracts of Avena Coleoptiles after Centrifugation

Tissue	Phytochrome ($\Delta\Delta A \times 10^3$)			% Pelletable Phytochrome
	Pellet	Supernatant	Total	
Dark*	1.5	29.6	31.1	4.8
Red‡	15.4	11.4	26.8	57.5

* Dark-grown, non-irradiated tissue.
‡ Dark-grown, light-treated tissue.

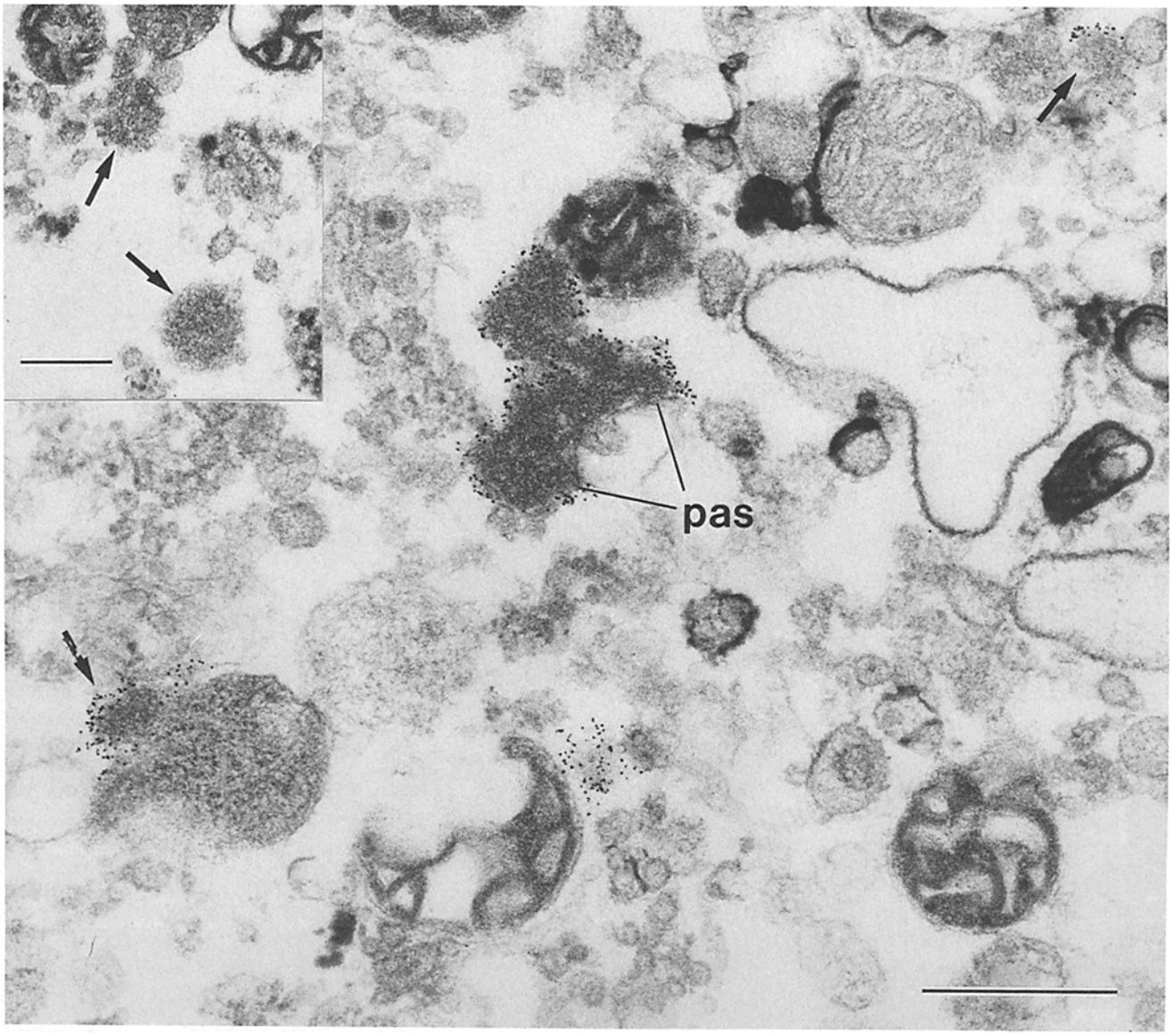

Figure 6. In vitro immunogold labeling of phytochrome as Pfr in a crude, pelletable fraction from *Avena* coleoptiles irradiated before their homogenization. PASs labeled with 5-nm colloidal gold are present as apparent aggregates (*pas*), or as individual structures (*arrows*) in these pellets. Bar, 0.5 μm. (*Inset*) Section from pellet incubated with non-immune mouse IgG. Structures (*arrows*) very similar to the PASs seen in the main micrograph are not labeled with gold. No other structures were immunolabeled. Bar, 0.3 μm.

vidually in each immunolabeling protocol (data not shown). It is unlikely that each monoclonal antibody would give rise to the same immunolabeling artifact, especially since they each bind to an independent epitope (4). Use of antigen-absorbed antibody is also a common control for immunocytochemistry. As noted above, however, since each monoclonal antibody has independently been shown to be directed to phytochrome, a monoclonal antibody preparation absorbed with phytochrome would no longer contain any antibody at all. Since this control is designed to detect the possible presence of contaminating antibodies in a polyclonal preparation, it therefore has no purpose when using highly purified monoclonal antibodies as we have done here. (*d*) Two quite different immunolabeling methods, namely in vitro and in vivo immunolabeling, including different methods of fixation and immunolabeling for the latter, gave essentially identical results. (*e*) R light induces a rapid and extensive intracellular redistribution of the antigen that is being recognized independently by each of the three monoclonal antibodies. This observation, together with the others summarized above, indicates that phytochrome is the only antigen being recognized.

The immunoelectron microscopic observations of sequestered phytochrome reported here are consistent with the conclusion from a recent time course study (11) that sequestering in *Avena* consists of two distinct but overlapping events. At the light microscope level, sequestering is characterized by an initial, rapid association of Pfr with numerous, discrete intracellular sites, each being <1 μm in size (11). This initial sequestration is followed by an apparent aggregation of these sites to form fewer, but larger, sites of sequestered phytochrome within the cell (11). The individual PASs seen in R/FR-irradiated tissue by electron microscopy (Figs. 2 *b*, 5) most likely correspond to the small, discrete

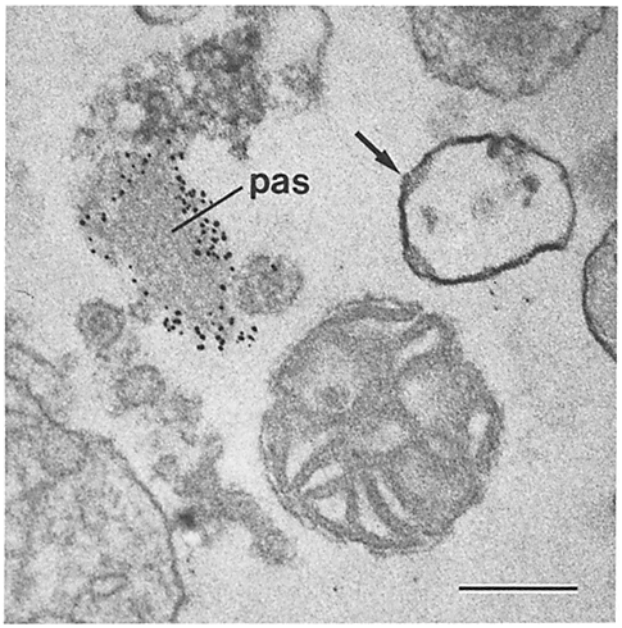

Figure 7. Carbohydrate staining of ultrathin sections of pelletable material from a crude extract of *Avena* coleoptiles irradiated before their homogenization. The immunolabeled PASs (*pas*) showed no detectable staining for carbohydrate. Other structures, presumably membrane fragments (*unlabeled arrow*), displayed the characteristic enhanced electron density that indicates a positive reaction for carbohydrate. Bar, 0.2 μm.

sites of Pfr localization detected earlier by immunofluorescence. The apparent aggregates of the PASs seen in Figs. 2 *a*, 3 *a*, 4 *a*, and 5 presumably represent the larger areas of sequestered phytochrome that become more prominent as the sequestering process proceeds (Fig. 2 *a*, inset; see also reference 11). The presence in the same cells of both individual and aggregated PASs is consistent with the intermediate stage of sequestering that is induced by the light treatment consisting of 1 s R light, 10 s darkness, and 4 s FR light (11).

The identity of the PASs in *Avena* coleoptiles is not evident. They have no morphologically recognizable membrane components. Initial cytochemical analysis indicates that they do not contain appreciable amounts of carbohydrate. The irregular conformations of the larger aggregates are unlike any structures of which we are aware in other plant cells. Since structures with morphology comparable to the PASs were not seen in dark-grown tissue that was not exposed to light, their presence in R/FR-irradiated tissue appears to be a consequence of irradiation. The amorphous, granular contents of the PASs indicate that they may be composed primarily of aggregates of protein. Such protein could be self-aggregates of Pfr, or possibly aggregates of Pfr and some other, as yet unidentified, protein(s). In this context, the distribution of the PASs throughout the plant probably reflects that of the chromoprotein itself (e.g., reference 15), as they are not evident in vascular cells (data not shown) that contain little if any phytochrome, but are present in the phytochrome-rich nodal tissue (15) of R/FR-irradiated *Avena* shoots (data not shown). The reports of R light–induced phytochrome sequestering in several other monocotyledonous species (7) and a dicotyledonous plant (23), as well as the widespread occurrence of R light–enhanced pelletability of phytochrome (16), indicates a potentially widespread occurrence of these PASs in higher plants.

The molecular basis of the association of Pfr with the PASs, and thus expression as either enhanced pelletability or sequestering, is not known. It has been suggested that both phenomena may represent a biologically important association of the chromoprotein with cellular membranes (e.g., reference 10). As noted above, however, the PASs identified here do not contain morphologically identifiable membranes (Fig. 5), indicating that this suggestion is not valid. Moreover, results from post-embedding immunolabeling (Figs. 3 and 4) indicate that phytochrome is within the PASs as well as on or near its surface, an observation that is inconsistent with an association of phytochrome with a membrane bounding the PASs. An attempt to determine whether sequestering might involve a well-defined domain on phytochrome was made by assaying sequestered phytochrome by immunofluorescence microscopy with a panel of 13 immunocytochemically competent monoclonal antibodies. Since all were able to detect sequestered phytochrome (data not shown), no evidence could be obtained to indicate that an epitope was being masked as a consequence of the association of phytochrome with the PASs. The antibodies tested, in addition to the three used above, were Oat-8, Oat-9, Oat-20, Oat-23, Oat-24, Oat-26, Oat-28, Oat-29, Oat-30, and Oat-31.

Nevertheless, as discussed elsewhere, both sequestering and pelletability exhibit characteristics consistent with a meaningful association between Pfr and a receptor (12, 13, 19). In particular, the rapidity of this association (11, 19) indicates that it may be an early event in the molecular mode of action of this pigment (see reference 19). However, other equally plausible alternatives exist. The PASs might represent intracellular sites where the Pfr-dependent dark destruction of phytochrome occurs (3). Alternatively, the PASs might act as vehicles to transport Pfr to intracellular sites, possibly to vacuoles, where dark destruction occurs. This latter possibility is consistent with the observations of Verbelen et al. (27), who suggested that the sequestering observed in *Avena* coleoptiles irradiated for 5 min with R light represents the association of Pfr with small, cytosolic vacuoles. Whatever their function, the occurrence of both sequestering and enhanced pelletability in a wide range of higher plants indicates that the PASs most likely have an important, although as yet unidentified, role in the biology of phytochrome-mediated photomorphogenic responses in higher plants.

This work was supported by National Science Foundation grants PCM-8315840 and PCM-8315882, and by a grant from the University of Georgia Research Foundation.

Received for publication 17 May 1986, and in revised form 7 August 1986.

References

1. Boeshore, M. L., and L. H. Pratt. 1980. Phytochrome modification and light-enhanced, in vivo–induced phytochrome pelletability. *Plant Physiol. (Bethesda).* 66:500–504.

2. Butler, W. L., and K. H. Norris. 1960. The spectrophotometry of dense light-scattering material. *Arch. Biochem. Biophys.* 87:31–40.

3. Butler, W. L., H. C. Lane, and H. W. Siegelman. 1963. Nonphotochemical transformations of phytochrome *in vivo*. *Plant Physiol. (Bethesda).* 38: 514–519.

4. Cordonnier, M.-M., H. Greppin, and L. H. Pratt. 1985. Monoclonal antibodies with differing affinities to the red-absorbing and far-red-absorbing forms of phytochrome. *Biochemistry.* 24:3246–3253.

5. Cordonnier, M.-M., C. Smith, H. Greppin, and L. H. Pratt. 1983.

Production and purification of monoclonal antibodies to *Pisum* and *Avena* phytochrome. *Planta.* 158:369–376.

6. De Mey, J., U. Moeremans, G. Geuens, R. Nuydens, and M. de Brabander. 1981. High resolution light and electron microscopic localization of tubulin with the IGS (immunogold staining) method. *Cell Biol. Int. Rep.* 5:889–899.

7. Epel, B. L., W. L. Butler, L. H. Pratt, and K. T. Tokuyasu. 1980. Immunofluorescence localization studies of the Pr and Pfr forms of phytochrome in the coleoptile tips of oats, corn and wheat. *In* Photoreceptors and Plant Development. J. De Greef, editor. Antwerpen University Press, Antwerpen. 121–133.

8. Lagarias, J. C. 1985. Progress in the molecular analysis of phytochrome. *Photochem. Photobiol.* 42:811–820.

9. Mackenzie, J. M., Jr., R. A. Coleman, W. R. Briggs, and L. H. Pratt. 1975. Reversible redistribution of phytochrome within the cell upon conversion to its physiologically active form. *Proc. Natl. Acad. Sci. USA.* 72:799–803.

10. Marmé, D. 1977. Phytochrome: membranes as possible sites of primary action. *Annu. Rev. Plant Physiol.* 28:173–198.

11. McCurdy, D. W., and L. H. Pratt. 1986. Kinetics of intracellular redistribution of phytochrome in *Avena* coleoptiles after its photoconversion to the active, far-red-absorbing form. *Planta.* 167:330–336.

12. Pratt, L. H. 1978. Molecular properties of phytochrome. *Photochem. Photobiol.* 27:81–105.

13. Pratt, L. H. 1979. Phytochrome: function and properties. *Photochem. Photobiol. Rev.* 4:59–124.

14. Pratt, L. H. 1984. Phytochrome purification. *In* Techniques in Photomorphogenesis. H. Smith and M. G. Holmes, editors. Academic Press, Ltd., London. 175–200.

15. Pratt, L. H., and R. A. Coleman. 1974. Phytochrome distribution in etiolated grass seedlings as assayed by an indirect antibody-labeling method. *Am. J. Bot.* 61:195–202.

16. Pratt, L. H., and D. Marmé. 1976. Red light–enhanced phytochrome pelletability: re-examination and further characterization. *Plant Physiol. (Bethesda).* 58:686–692.

17. Pratt, L. H., J. E. Wampler, and E. S. Rich, Jr. 1985. An automated dual-wavelength spectrophotometer optimized for phytochrome assay. *Anal. Instrum.* 13:269–287.

18. Quail, P. H. 1978. Irradiation-enhanced phytochrome pelletability in *Avena:* pigment release by Mg^{2+}-gradient elution. *Photochem. Photobiol.* 27: 759–765.

19. Quail, P. H. 1983. Rapid action of phytochrome in photomorphogenesis. *In* Encyclopedia of Plant Physiology, New Series. Vol. 16. W. Shropshire and H. Mohr, editors. Springer-Verlag, Berlin. 178–212.

20. Quail, P. H., and W. R. Briggs. 1978. Irradiation-enhanced phytochrome pelletability: requirement for phosphorylative energy *in vivo. Plant Physiol. (Bethesda).* 62:773–778.

21. Quail, P. H., D. Marmé, and E. Schäfer. 1973. Particle-bound phytochrome from maize and pumpkin. *Nature New Biol.* 245:189–191.

22. Raikhel, N. V., M. Mishkind, and B. A. Palevitz. 1984. Immunocytochemistry in plants with colloidal gold conjugates. *Protoplasma.* 121:25–33.

23. Saunders, M. J., M.-M. Cordonnier, B. A. Palevitz, and L. H. Pratt. 1983. Immunofluorescence visualization of phytochrome in *Pisum sativum* L. epicotyls using monoclonal antibodies. *Planta.* 159:545–553.

24. Shropshire, W., Jr., and H. Mohr, editors. 1983. Encyclopedia of Plant Physiology, New Series, Volume 16. Springer-Verlag, Berlin. 832 pp.

25. Taylor, J. W., and M. S. Fuller. 1981. The Golgi apparatus, zoosporogenesis, and development of the zoospore discharge apparatus of *Chytridium confervae. Exp. Mycol.* 5:35–59.

26. Thiéry, J.-P. 1967. Mise en évidence des polysaccharides sur coupes fines en microscopie électronique. *J. Microsc. (Paris).* 6:987–1018.

27. Verbelen, J.-P., L. H. Pratt, W. L. Butler, and K. Tokuyasu. 1982. Localization of phytochrome in oats by electron microscopy. *Plant Physiol. (Bethesda).* 70:867–871.